Natural Science Report, Ochanomizu University, Vol. 34, No. 2, 1983
お茶の水女子大学 自然科学報告 第34巻 第2号

Laboratory Simulation of Turbulent Flow in the Lower Part of the Planetary Boundary Layer

Shigeru Nemoto and Noriko Konda

Environmental Science, Faculty of Science, Ochanomizu University, Tokyo
(Received September 7, 1983)

Abstract

The vertical distribution of horizontal mean wind velocity is approximately described by the power law in the lower atmosphere. In the present paper, a method of intentionally constructing a grid by satisfing an empirical formula between an exponent n of wind profile and grid parameters is proposed and it is also shown that the model wind produced by this method is similar fairly well to the natural wind observed at Minnesota on vertical distributions of horizontal mean wind velocities and turbulent intensities, while vertical distributions of their vertical fluxes of momentum are not similar to each other. However, it is shown that possibility of simulating the last ones of the above-mentioned characteristics by suitable combination of grid parameters is expected.

§ 1. Introduction.

Simulation of turbulent flows between natural wind in a field and model wind in a wind tunnel includes the intensities, spectra of the individual components of turbulence and their higher order correlations (Reynolds stress or momentum flux) as well as the mean flow patterns.

A complete simulation of the above wind characteristics is difficult and partial models of wind, as a result, have commonly been used. To data, following approaches have been taken:

(1) Curved screens (Baines, 1963), grids of horizontal rods placed at a varying spacing (Owen and Zinkiewicz, 1957) and grids of horizontal scantlings placed at a varying spacing (Adachi and Kato, 1973) have been used to model the structure of the mean wind and obtain information on time-average flow characteristics as well as mean structure response. Methods employing graded blockage, grids of rods or slats, etc. have been used by Sato et al. (1974) and by Ogawa (1976, 1981).

(2) Coarse grids have been used by a number of researchers, in particular, Baines and Peterson (1950), Vickery (1965), Surry (1967) and others, to produce large scale turbulence superimposed on a uniform flow.

(3) Grids of flat plates with added turbulence generators (Lloyd, 1967) and vortex generator (Armitt, 1966), have been used to model both mean and turbulence characteristics. The most popular of the passive devices is the barrier/vortex generator/roughness system developed by Counihan (1969).

(4) Turbulent boundary layer tunnels have been used to model wind, in particular, by Bailey and Vincent (1943), by Jensen (1958), by Nemoto (1968), at Colorado State University (Cermak, 1958; Plate and Cermak, 1963) and at the University of Western Ontario (Davenport and Isyumov, 1968).

(5) Schon and Mery (1971) injected air perpendicular to the flow through a porous plate at the entrance to the test section. Nagib et al. (1974) have added some flexibility to the Schon et al. technique.

However, in spite of the use of various kinds of grids, it seemed for us that no available relationship between grid parameters and characteristics of turbulent flow generated by it have been obtained, hence it was impossible to intentionally simulate the natural wind in the field.

In the present paper, a method of intentionally constructing the grid which realizes the vertical distributions of mean wind velocity and turbulent intensity to be desired is first proposed and the model wind generated by this method is compared with the natural wind.

§ 2. Objective.

The aim of this study is establishment of the practical method by which the turbulent flow in the lower part of the planetary boundary layers is similarly and intentionally reproduced in the wind tunnel with very short range of test section. If the method is found, it is expected that the intensities, spectra of the individual components of turbulence, their higher order correlations and the mean flow patterns of natural local wind become similar to those of the model wind in the wind tunnel.

§ 3. Wind tunnel experiments.

3.1 Construction of the grid for making vertical wind profile in the lower part of the planetary boundary layer similar to that of its model wind in the wind tunnel

The wind tunnel of the type of Göttingen was used and its test section had dimension of 70 cm×70 cm×200 cm (height×width×length). The vertical distribution of horizontal mean wind velocity U is usually expressed by the logarithmic profile up to several tens meters above the ground surface in the neutral state and the exponential profile holds in the layer higher than that. However, it is here supposed that the exponential wind profile in the form of $U \propto z^n$ is applicable to the whole layer in question, that is, from the ground surface to a few hundreds meters in height.

The exponential wind profile in the wind tunnel was produced in the following way. That is, the grid of alminum angle (L-shaped alminum, it is, for convenience, called only angle hereafter) placed at a varying spacing was used as shown in Fig. 1. The grid was constructed so that any spacing d_{m-1} between the m-th angle and the $(m+1)$-th one might be expressed by an exponential

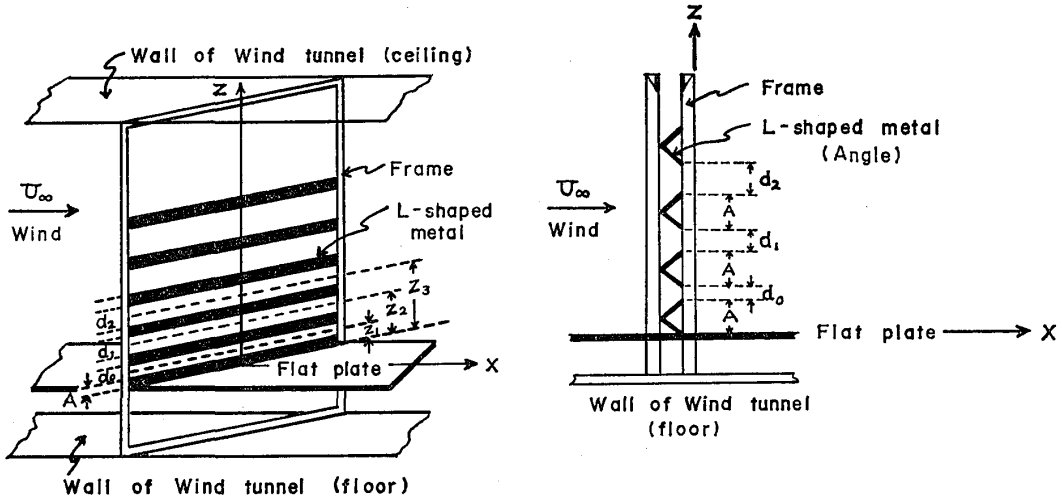

Fig. 1. Grid constructed with angles, which shows the case of regular direction of angle.

function of height (z_m) from the flat plate to the center of spacing d_{m-1}. Therefore, the equation

$$\log z_m=\alpha \log d_{m-1}+\beta$$

holds between d_{m-1} and z_m, and as seen from Fig. 1 β is expressed as

$$\beta=\log z_1-\alpha \log d_0=\log \frac{z_1}{d_0^\alpha}$$

hence the equation

$$z_m=\left(\frac{d_{m-1}}{d_0}\right)^\alpha\left(A+\frac{d_0}{2}\right) \tag{1}$$

can be obtained, where

A: effective width of angle
d_0: initial spacing, that is, spacing between the bottom angle and the next one
α: $d(\log z)/d(\log d)$

On the other hand, there is the following relation between spacing d_{m-1} and its height z_m, that is,

$$z_m=mA+\sum_{i=0}^{m-1} d_i-\frac{d_{m-1}}{2} \tag{2}$$

Therefore, from equation (1) and equation (2), the equation

$$\left(\frac{d_{m-1}}{d_0}\right)^\alpha(2A+d_0)=2\left(mA+\sum_{i=0}^{m-1} d_i\right)-d_{m-1} \tag{3}$$

can be derived. Hence, in equation (3), when A, d_0 and α are given and value of m varies from 1 to $(m-1)$, each spacing d_{m-1} corresponding to each value of m can be successively obtained by the use of a personal computer (NEC, PC-8800) and the grid to be desired can be constructed.

Furthermore, for the case of two dimensional turbulent flow an exponent n of wind profile is considered to be a function of A, α, d_0, x and U_∞ (uniform

tunnel velocity). We, hence, next try to determine the form of the above function experimentally. Wind profiles were measured at x=80, 100, 120 and 140 cm for wind velocities U_∞=0.8~1.6 m/sec, where x is distance downwind from the grid. These results show that the wind profile at x=140 cm does not differ from that at x=120 cm, although wind profiles at x=80, 100 cm differ from location to location due to the lack of development of turbulence and further the wind profile is almost independent of wind velocity within the above-mentioned region of wind velocity (in the case of pipe grids this holds for U_∞=1, 1.5, 2, 2.5 m/sec). Therefore in the present work all the measurements were carried out under the conditions of x=120 cm and U_∞=1.5 m/sec.

3.2 Measurement of wind velocity components and data processing

Wind velocity components were obtained by constant-temperature hot-wire anemometry. That is, a hot-wire anemometer with X-shaped probe (diameter of wire: 5 μm, length of wire: 2 mm) was used for measurement of x and z components of wind velocity. The outputs of the anemometer, that is, fluctuating wind velocity components in the streamwise and vertical directions were recorded on magnetic tapes with a data recorder. The play back outputs of the data recorder were processed by an analog data analyzer, which were consisted of power supply unit, mean meter unit, sigma meter unit, five band-pass sigma meter units and flux meter unit (for further details the reader may refer to Yasueda et al., 1980 and Kato, 1982) and furthermore a spectrum analyzer and FFT were used.

The following items were examined on the basis of data mentioned above:

(1) Determination of an empirical formula for n under the conditions that it is independent of x and U_∞, that is, determination of the functional form of $n=F(A, \alpha, d_0)$
(2) Vertical distribution of turbulent intensity
(3) Variation of spectral scales of u and w components of turbulence with height
(4) Vertical distribution of vertical flux of momentum

and the results obtained will be described in the following chapter.

§ 4. Results of experiments.

4.1 Vertical distribution of horizontal mean wind velocity

Fig. 2 shows three vertical distributions of horizontal mean wind velocity U for each case of d_0=5, 13, 25 mm, where the effective width of angle A=13.4 mm, U_∞=1.5 m/sec, distance downwind from the grid x=120 cm and α=5. It is seen from this figure that the wind profile in the case of d_0=5 mm slightly slants to the right hand side above a height of 140 mm, in the case of d_0=13 mm the wind profile is approximately expressed by a straight line over all the heights dealt with here and in the case of d_0=25 mm the wind profile slightly slants to the left hand side above a height of 120 mm. That is, the upper part of the

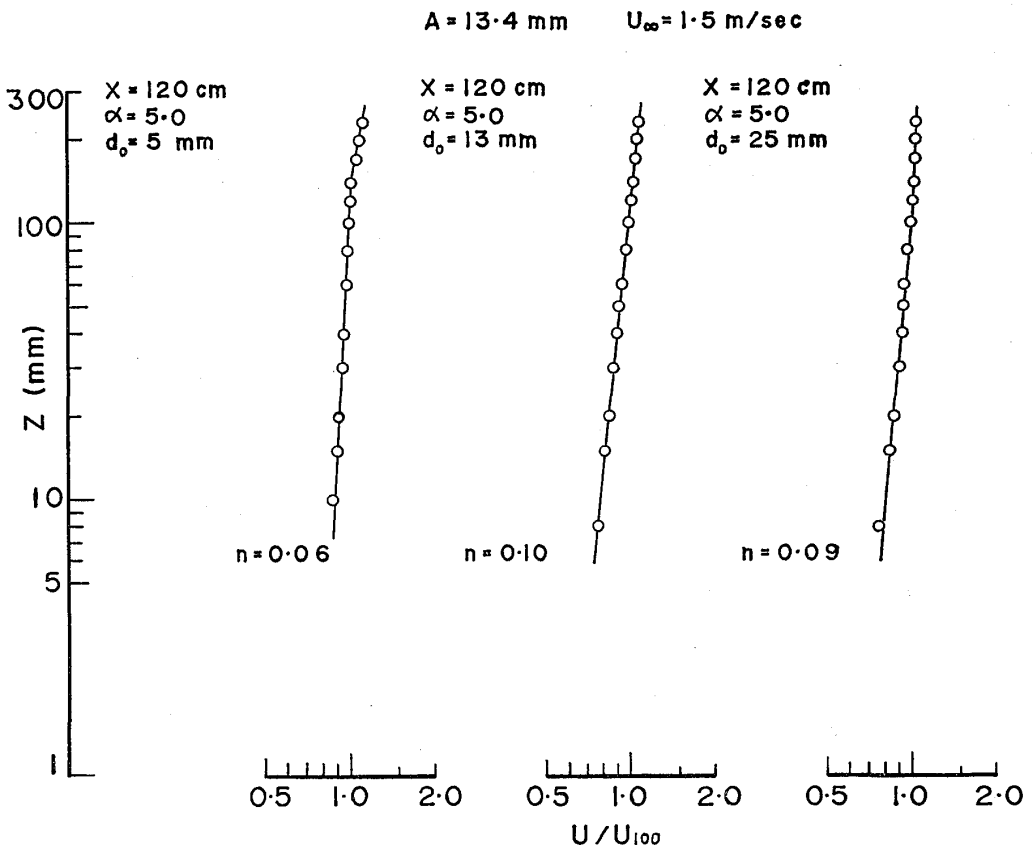

Fig. 2. Vertical distribution of horizontal mean wind velocity for d_0=5, 13, 25 mm in the case of U_∞=1.5 m/sec, x=120 cm and α=5.

wind profile tends to slant successively to the left hand side as d_0 increases. In this figure horizontal mean wind velocity U is normalized with the wind velocity U_{100} at the reference height of 100 mm.

4.2 Empirical formulas expressing the relation between exponent n of wind profile and grid parameters

It is here considered that the exponent n is a function of A, α and d_0 as already mentioned. Therefore we next try to find the empirical formula for n. In this case, the following two cases are considered:

(1) the case where the corner of the angle is faced to the windward (hereafter this case is called the case of regular direction of angle)
(2) the case where the corner of the angle is faced to the leeward (hereafter this case is called the case of reversed direction of angle)

All the figures in the present paper show the results obtained in the case of regular direction of angle as shown in Fig. 1, except for the lower part of Fig. 6. At first we investigate variation of n with d_0 for each case of α=3, 4, 5, 7, 10. These results are shown in the upper parts of Figs. 3-1, 3-2 and 3-3. In these figures the ordinate indicates exponent n and the abscissa indicates initial spacing d_0 normalized by the effective width of angle A. It is found from these figures

that n decreases until about $d_0/A=0.5$ and on the contrary increases for d_0/A larger than that, that is, variation of n with d_0/A takes a V-shaped one. However, turbulent intensities are very small for the increasing part, that is, for the right hand side part of the V-shaped variation as shown later and such a small turbulent intensity can usually not be found on the land. Therefore, we here deal with only the decreasing part, that is, the left side one. It is then found that n for all the left side part is expressed by the following equation, that is,

$$n=(0.055-0.0042\alpha)\left(\frac{d_0}{A}\right)^{-(0.11+0.103\alpha)} \tag{4}$$

and the conditions of application of the above equation are

$$\alpha<13, \quad 0.15\leqq\left(\frac{d_0}{A}\right)\leqq 0.45$$

The lower parts of these figures show variation of the upper height (h) of the layer up to where the power law of the wind profile approximately holds from the flat plate. The exponent n can be obtained by suitable combination of α and d_0 after A being determined, but in this case this combination must be chosen in

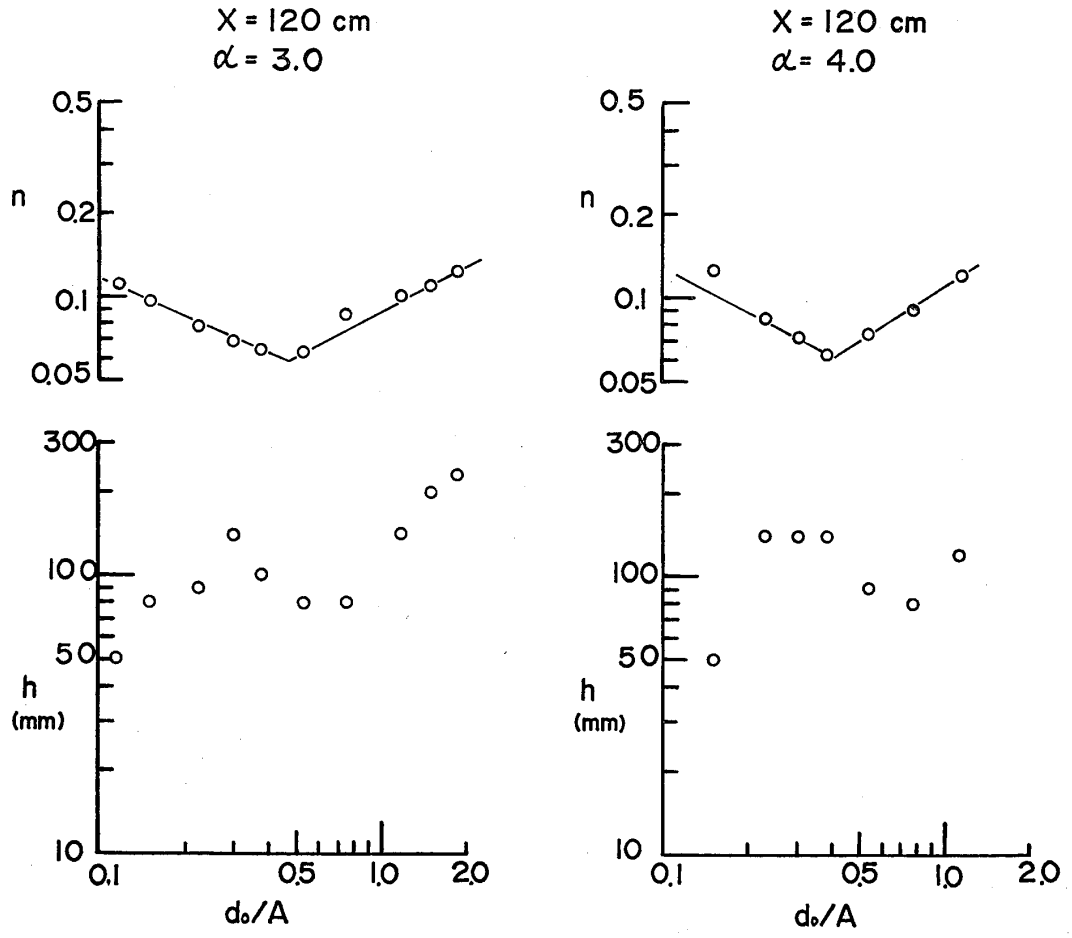

Fig. 3-1. The upper figures show variations of exponent n with normalized initial spacing d_0/A for $\alpha=3$ and 4. The lower figures show variations of the upper limit of the power law close to the flat plate with d_0/A.

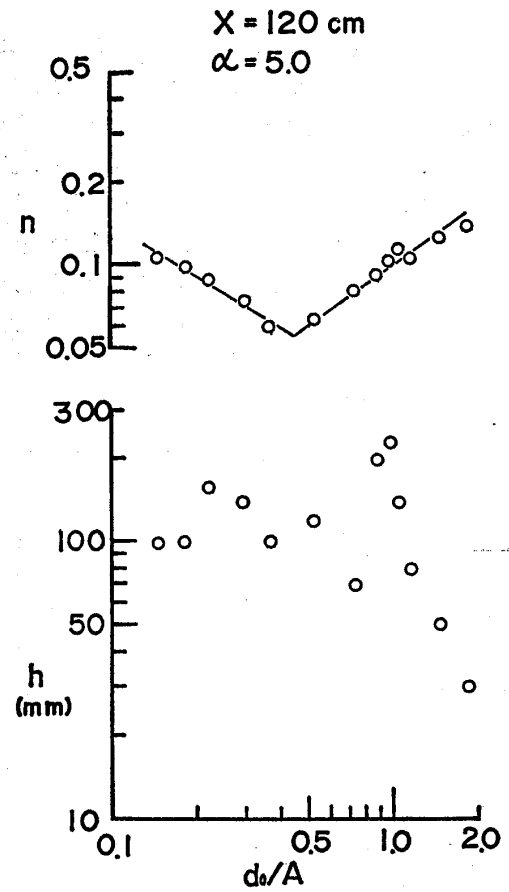

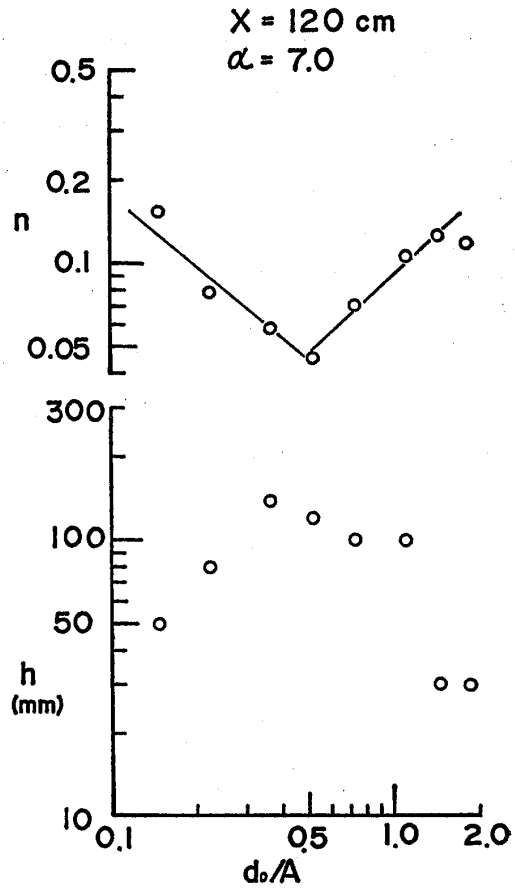

↖ Fig. 3-2. The same as Fig. 3-1 except for $\alpha=5$ and 7.

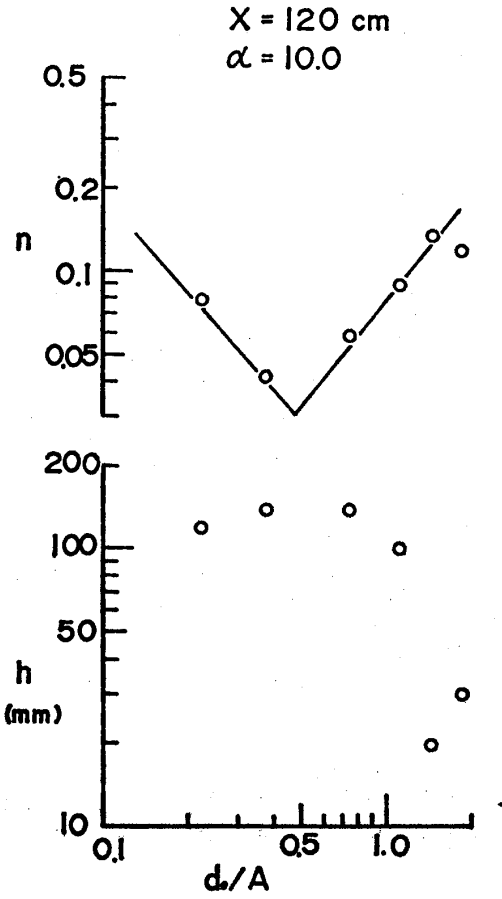

← Fig. 3-3. The same as Fig. 3-1 except for $\alpha=10$.

order that the turbulent intensities may agree with those of natural wind at each corresponding height. However, it is found from the experimental results shown later that the turbulent intensities are mainly dependent of d_0 and almost independent of α except for the cases of $d_0 \leqq 2.0$ mm. Therefore, we first choose d_0 for which the turbulent intensities in the model wind agree with those in the natural wind and then choose α for which n takes a value to be expected, where for determination of this value of α equation (4) is used, and at last by determining spacing of adjacent angles by equation (3) each spacing can be successively obtained from the initial spacing. The grid to be desired thus can be constructed successively from the bottom.

On the other hand, for the case of reversed direction of angle the following empirical formula can be obtained, that is,

$$n=(0.034-0.0015\alpha)\left(\frac{d_0}{A}\right)^{-(0.65+0.098\alpha)} \tag{5}$$

and the conditions of application of the above equation are

$$\alpha<22, \quad 0.1\leqq\left(\frac{d_0}{A}\right)\leqq 0.5$$

Another case is that of a pipe grid (Y. Tanaka and Y. Matsuda, unpublished) and for this case the equation

$$n=(0.048-0.0053\alpha)\left(\frac{d_0}{A}\right)^{-(0.57+0.08\alpha)} \tag{6}$$

is obtained and the conditions of application of this equation are

$$\alpha<9, \quad 0.18\leqq\left(\frac{d_0}{A}\right)\leqq 0.25$$

4.3 Vertical distributions of turbulent intensities

Vertical distributions of the turbulent intensities of u-component for $\alpha=3$, 5, 7 at $x=120$ cm are shown in Figs. 4-1, 4-2 and 4-3. In these figures the ordinate indicates nondimensional height (z/A) and the abscissa indicate turbulent intensity of u-component of wind velocity $(\sqrt{\overline{u'^2}}/U)$. It is seen from these figures that $\sqrt{\overline{u'^2}}/U$ is small for $d_0\geqq 10$ mm or $d_0/A\geqq 0.75$. Incidentally, values of turbulent intensities in the case of regular direction of angle are, in average, 1.37 times as large as those in the case of reversed direction of angle for $d_0=3$ mm and 1.26 times as large as for $d_0=5$ mm. On the other hand values of turbulent intensities of w-component in the case of regular direction of angle are 1.21 times as large as those in the case of reversed direction of angle for $d_0=3$ mm, but they have the same value for $d_0=5$ mm, furthermore each value for u and w components is independent of height within the height range in question for the case of $d_0\geqq 13$ mm, which is out of application of equation (4).

4.4 Variations of spectral scales with height

Variations of spectral scales λ_{up} and λ_{wp} with height are shown in Fig. 5. In this figure the ordinate indicates spectral scale and the abscissa indicates

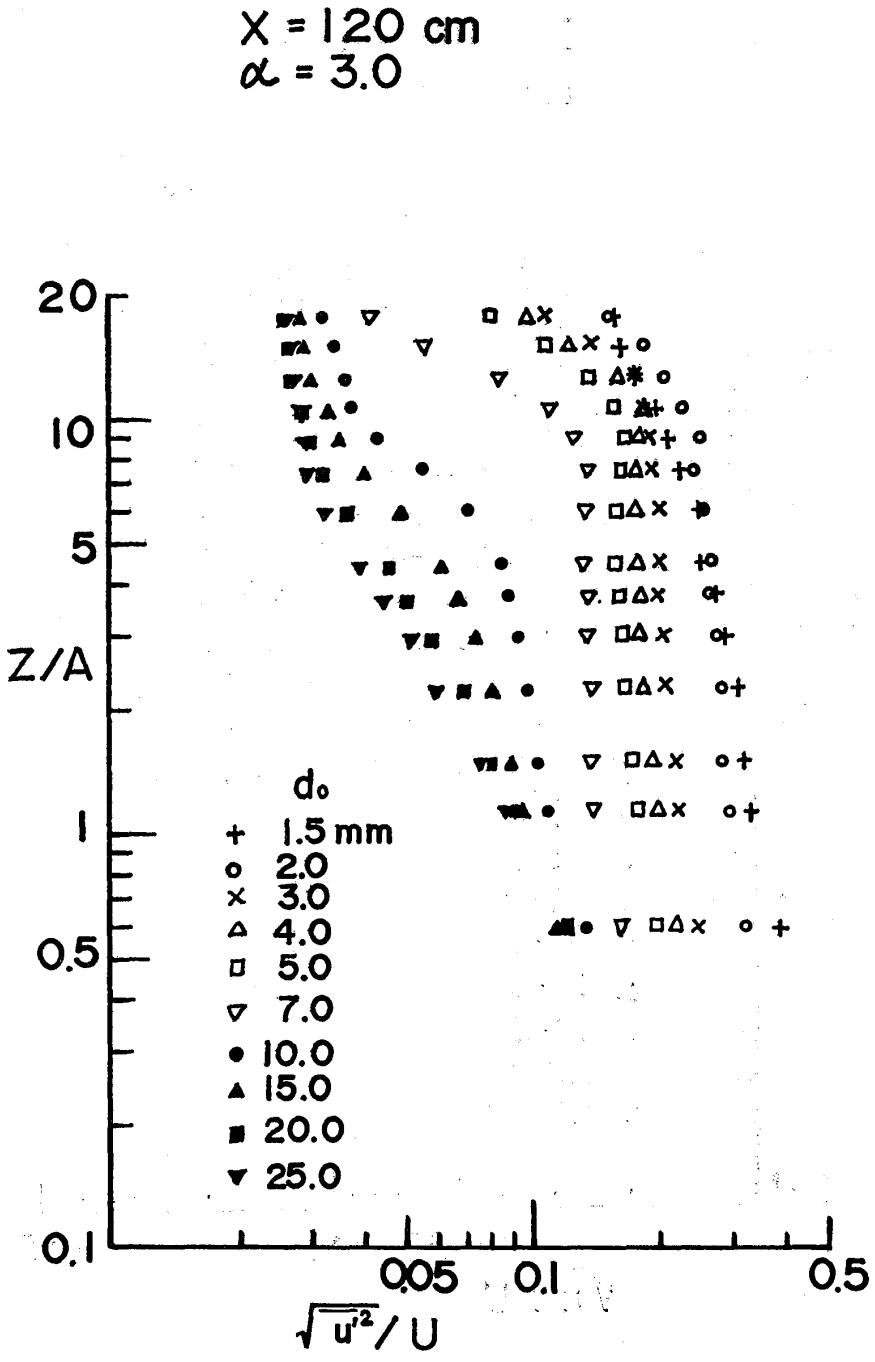

Fig. 4-1. Variation of vertical distribution of turbulent intensity $\sqrt{u'^2}/U$ with initial spacing d_0 for $\alpha=3$.

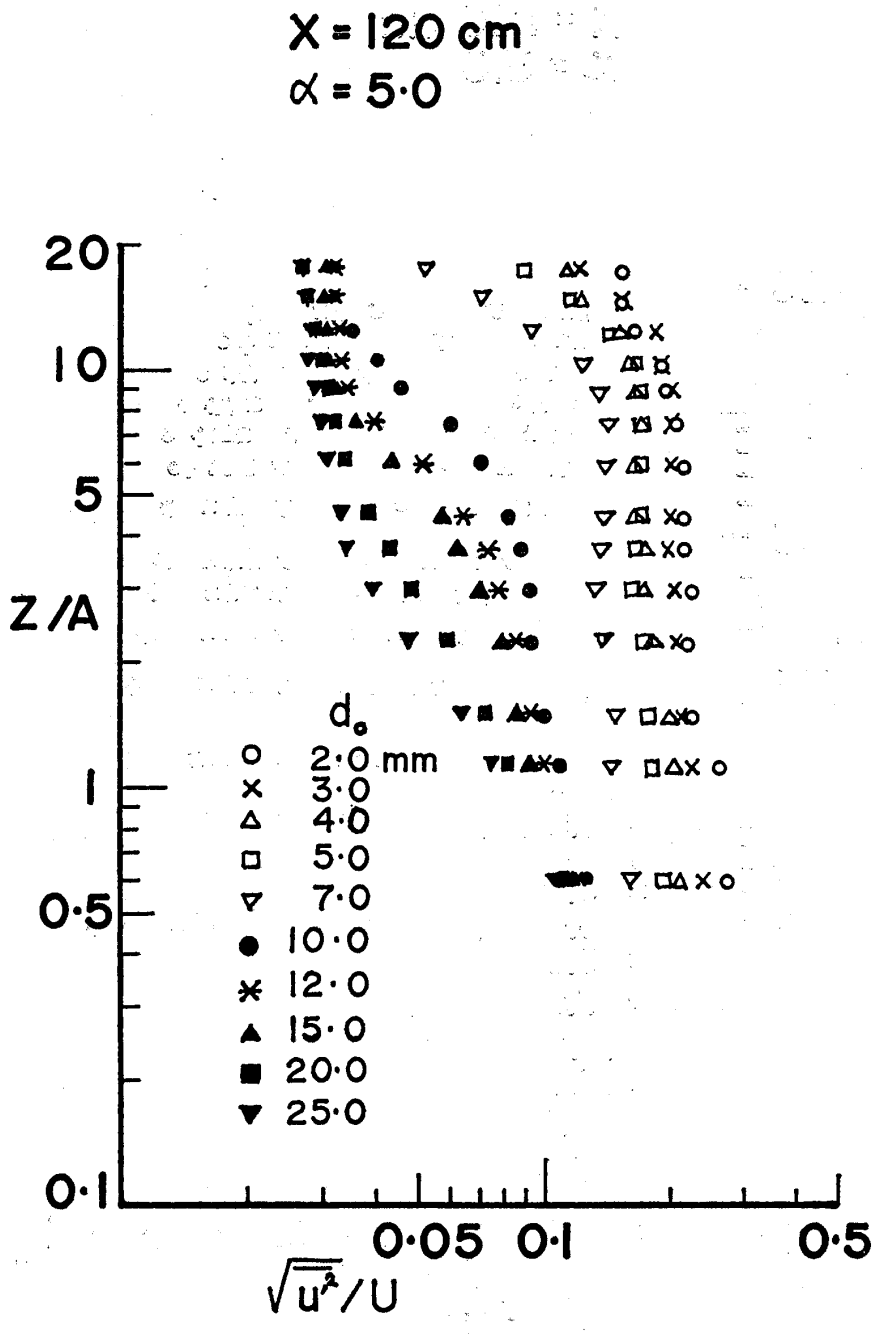

Fig. 4-2. The same as Fig. 4-1 except for $\alpha=5$.

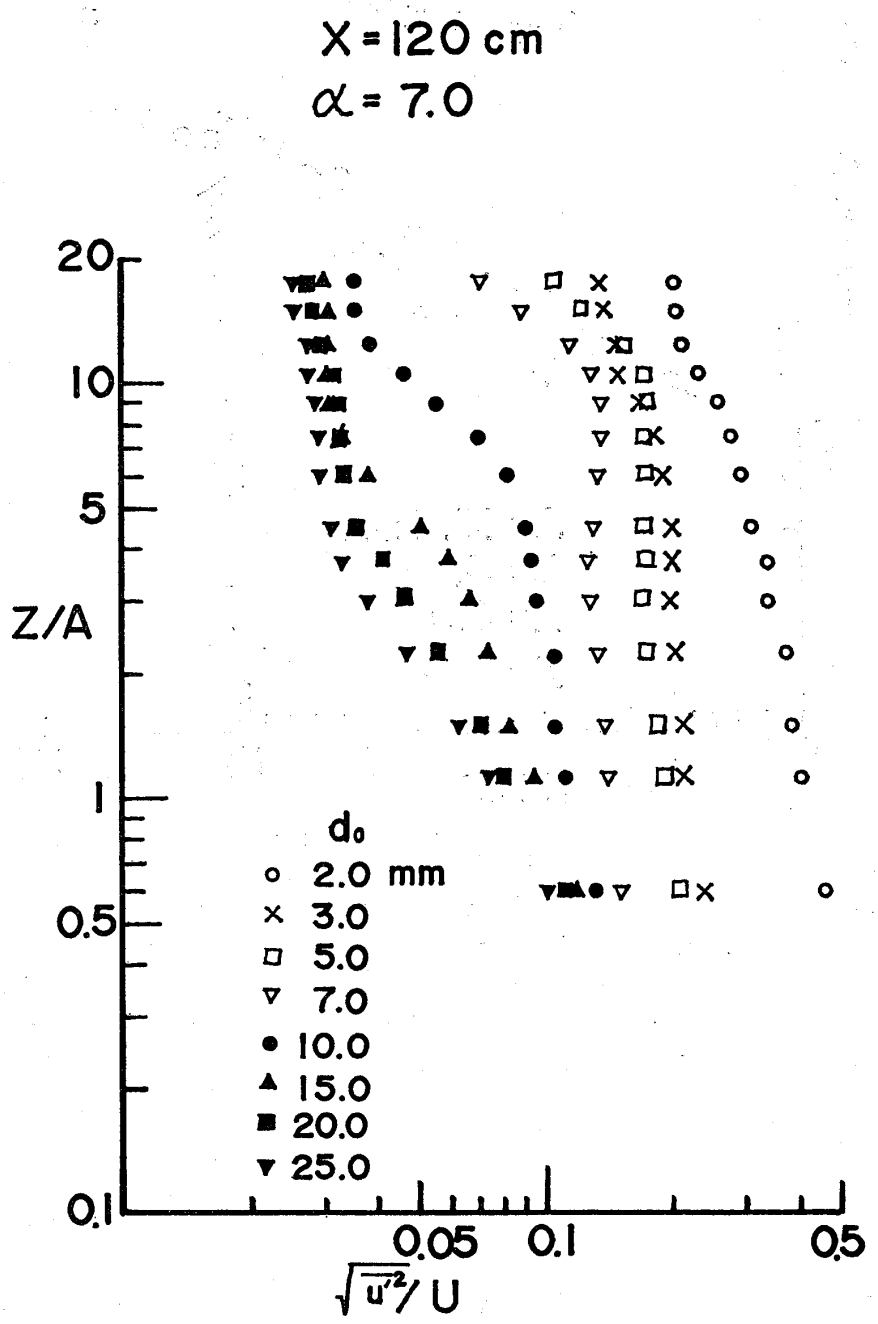

Fig. 4-3. The same as Fig. 4-1 except for $\alpha=7$.

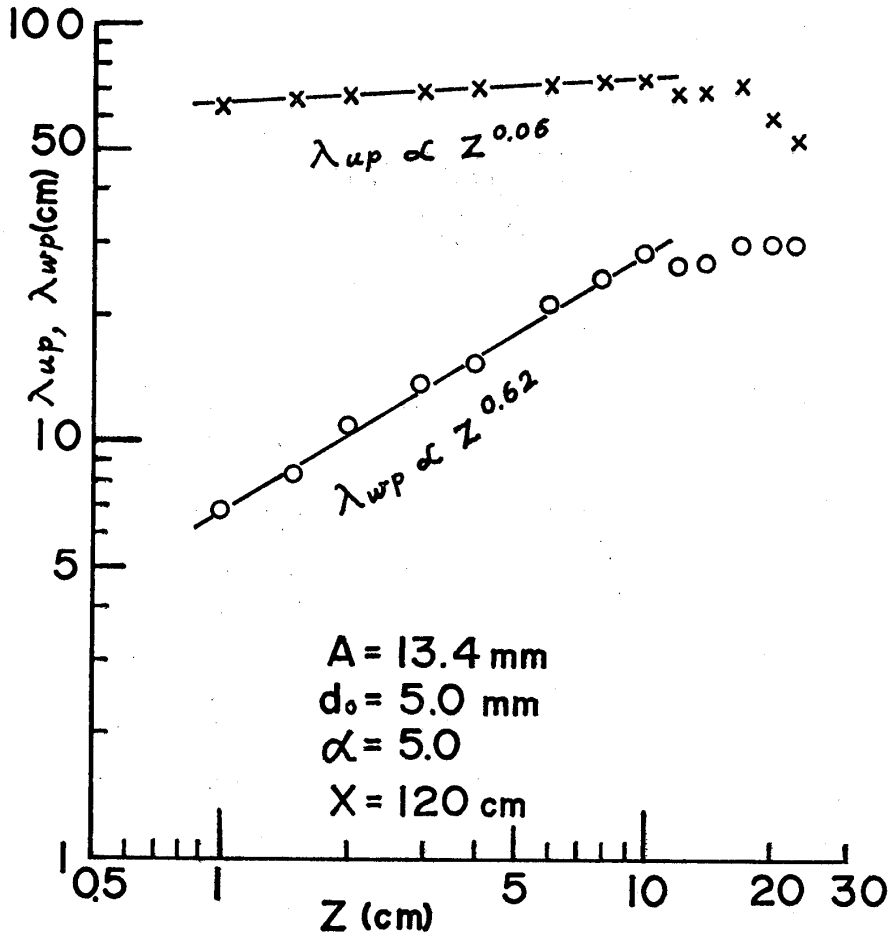

Fig. 5. Variations of spectral scales λ_{up} and λ_{wp} with height.

height and the upper curve shows the variation of λ_{up} with height and the lower one shows that of λ_{wp}. Here λ_{up} means the scale of turbulence corresponding to a peak frequency of power spectrum of u-component of turbulence and λ_{wp} means that corresponding to a peak frequency of power spectrum of w-component. It is an experimental result for the case of $A=13.4$ mm, $d_0=5.0$ mm, $\alpha=5$, $x=120$ cm and $U_\infty=1.5$ m/sec. As seen from this figure the following relationships are obtained:

$$\lambda_{up} \propto z^{0.06}$$

$$\lambda_{wp} \propto z^{0.62}$$

for z from 1 cm to 10 cm, and each value tends to be constant for z larger than 10 cm. Unfortunately these results can not be compared with those at Minnesota, because no relation is obtained between spectral scale and height. However it seems that the value of exponent of z for the spectral scale λ_{up} is one order of magnitude smaller as compared with other field observation with a tower (e.g. Hanafusa et al., 1981).

On the other hand, comparison of height variation of λ_{up} and λ_{wp} for the two directions of angle has been made. In these experiments d_0 is varied from 3 mm to 13 mm under the condition of $A=13.4$ mm, $\alpha=5$, $x=120$ cm and $U_\infty=1.5$

m/sec. The results of experiments are summarized as follows:

(1) Variation of λ_{up} with height for the case of regular direction of angle: Each value of λ_{up} at each height increases as d_0 decreases and the rate of variation of λ_{up} with height $d\lambda_{up}/dz$ tends to decrease as d_0 decreases.

(2) Variation of λ_{up} with height for the case of reversed direction of angle: Each value of λ_{up} at each height increases as d_0 decreases in the same manner as (1), but the trend of variation of $d\lambda_{up}/dz$ with d_0 is not obvious.

(3) Variation of λ_{wp} with height for the case of regular direction of angle: Each value of λ_{wp} at each height increases as d_0 decreases and $d\lambda_{wp}/dz$ tends to increase as d_0 decreases.

(4) Variation of λ_{wp} with height for the case of reversed direction of angle: Each value of λ_{wp} at each height increases as d_0 decreases in the same manner as in (3), and $d\lambda_{wp}/dz$ tends to increase as d_0 decreases, but the rate of variation is not so large as in (3).

As an example, variation of λ_{wp} with height in the two cases of regular and reversed directions of angle are shown in Fig. 6 and the conditions of experiments are shown in the figure.

It is seen from these results (***4.3*** and ***4.4***) that the grid of regular direction of angle is more effective than the grid of reversed direction of angle to produce the turbulent flow with larger intensity of turbulence.

§ 5. Comparison of the result measured in the wind tunnel with that observed in the lower atmosphere.

Comparison of the result observed by the use of a kite balloon at Minnesota (1976) with that measured in the wind tunnel is shown in Fig. 7. The ordinate in the left hand side indicates height for the model wind and that in the right hand side height for the natural wind. A vertical distribution of horizontal mean wind velocity is shown in the left hand side of the figure and the abscissa indicates each horizontal mean wind velocity U normalized with each velocity U_{100} at each reference height of $z_m=100$ mm and $z_n=100$ m (suffix m denotes that its quantity is refered to model experiment and suffix n natural wind). Experimental conditions in the wind tunnel and meanings of each sign are shown in the figure respectively.

The middle figure shows comparison of vertical distributions of turbulent intensities $\sqrt{\overline{u'^2}}/U$ and $\sqrt{\overline{w'^2}}/U$ between model wind and natural local one. It is found from the figure that the distribution up to $z_m=150$ mm in the wind tunnel experiment agree fairly well with that observed at Minnesota up to $z_n=150$ mm.

The figure in the right hand side shows the vertical distributions of normalized vertical flux of momentum $(-\overline{u'w'}/U^2)$. It is seen from this figure that the two vertical distributions do not agree with each other. Therefore, if we hope simulation of these vertical fluxes of momentum, we must try to find more suit-

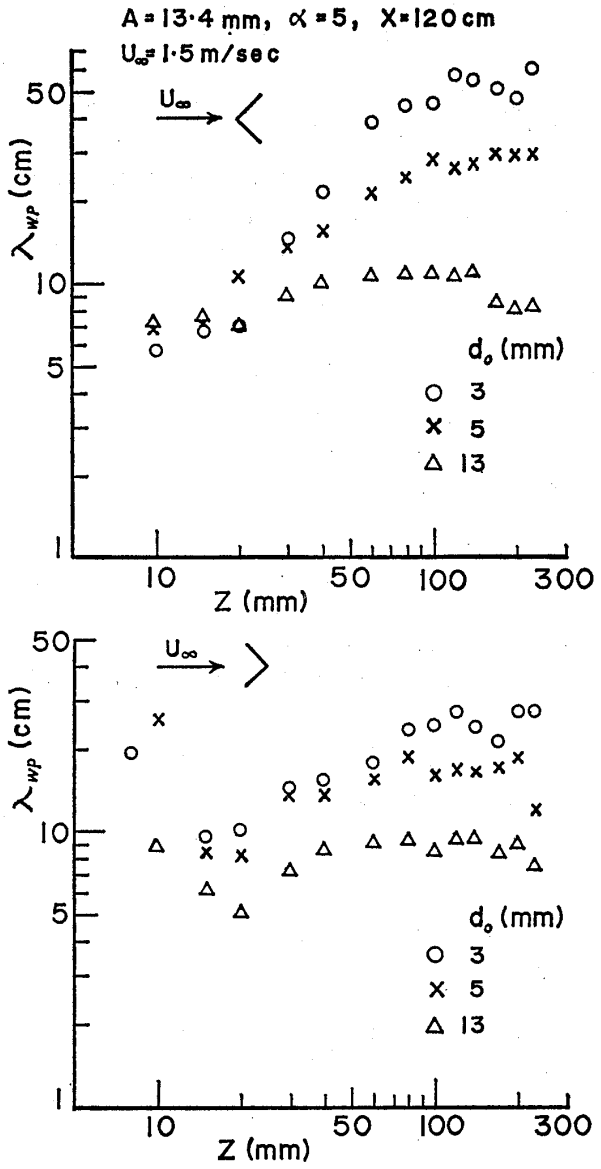

Fig. 6. Variations of spectral scale λ_{wp} with height for d_0=3, 5, 13 mm. The upper figure shows the case of regular direction of angle and the lower one shows the case of reversed direction of angle.

able combination of parameters A, α and d_0.

It is usually considered that if the two conditions, that is, the agreement of the vertical profiles of mean wind velocity and that of turbulent intensity, are satisfied at each corresponding location of model and prototype, the two turbulent fields becomes similar, but if the agreement of momentum flux is further required, the experiment with a higher degree of accuracy is necessary. It is found from the above-mentioned description that the results obtained at Minnesota is simulated in the wind tunnel in a scale of 1/1000 only for both vertical distributions of mean wind velocity and of turbulent intensity up to z_n=150 m. This is due to difference in sensitivity among vertical distributions of mean wind velocity, of turbulent intensity and of momentum flux. The vertical distribution of mean

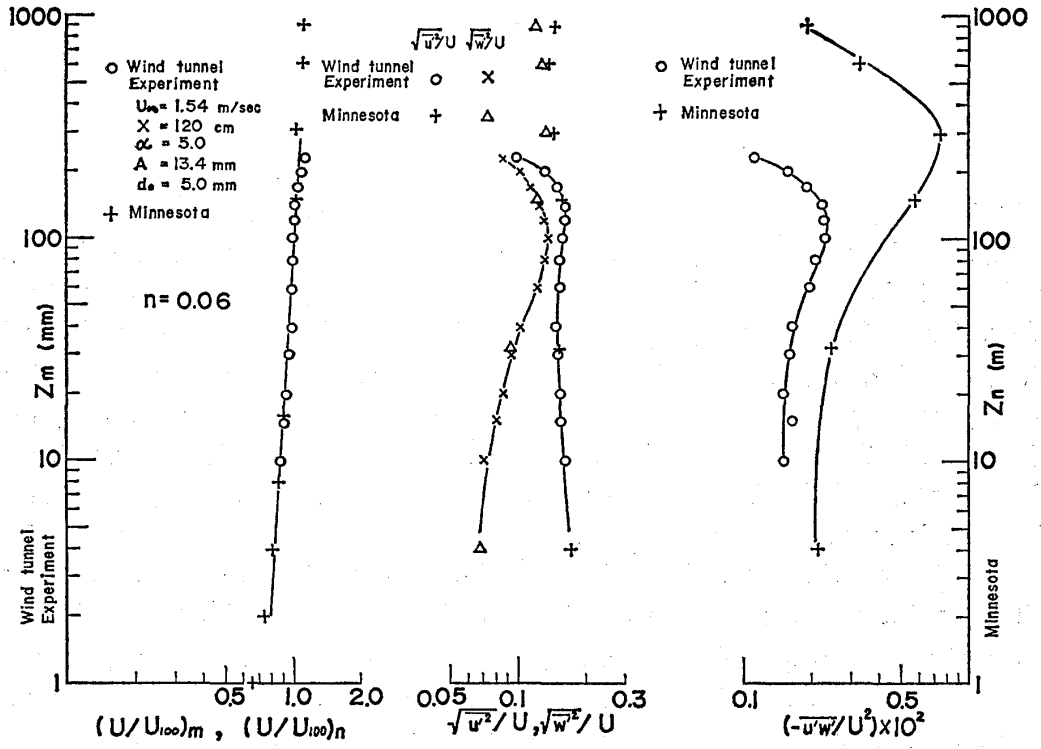

Fig. 7. Comparison of the results measured in the wind tunnel with those observed at Minnesota (The left side figure shows the wind profiles, the middle one vertical distributions of turbulent intensities $\sqrt{\overline{u'^2}}/U$ and $\sqrt{\overline{w'^2}}/U$ and the right side one vertical distribution of vertical fluxes of momentum).

wind velocity is most insensitive to variation of grid parameter and then that of turbulent intensity. The vertical distribution of momentum flux is more sensitive.

§ 6. Comparison of the two turbulent flows behind two grids with different effective width of angle.

The two measurements, that is, case 1 and case 2, were made at $x=120$ cm for $U_\infty=1.54$ m/sec. Each value of parameters in case 1 is as follows:

$$A=13.4\text{ mm}$$

$$d_0=5.0\text{ mm}$$

$$\alpha=5.0$$

$$n=0.06$$

We next construct a grid with the effective width of 13.9 mm, but in this case we use the same values as in case 1 for parameters α and n. If we calculate d_0 under the above conditions by using the empirical formula (4), we can obtain 5.47 mm as a value of parameter d_0, that is, construct the grid with the following parameters

$$A=13.9\text{ mm}$$

$$d_0=5.47\ \text{mm}$$

$$\alpha=5.0$$

$$n=0.06$$

and call it case 2.

The results obtained by using these two grids (case 1 and case 2) are shown in Fig. 8. The figure in the left hand side shows the two normalized wind profiles. It is seen from the figure that two wind profiles agree well with each other. The middle figure shows the vertical distributions of turbulent intensities $\sqrt{\overline{u'^2}}/U$ and $\sqrt{\overline{w'^2}}/U$. In this figure the distributions of turbulent intensity of u-component agree well with each other but those of w-component slightly differ. The figure in the right hand side shows the vertical distributions of vertical flux of momentum. It is obviously seen from the figure that the two profiles are far different from each other and the distribution observed at Minnesota will be in the middle of the two. Therefore, if the angle with the effective width of a suitable value between 5.0 mm and 5.47 mm is used, it may be expected that we can make each of n, $\sqrt{\overline{u'^2}}/U$, $\sqrt{\overline{w'^2}}/U$ and momentum flux $(-\overline{u'w'}/U^2)$ of the two cases, that is, model wind and natural local wind (in this case the result observed at Minnesota) agree fairly well with each other.

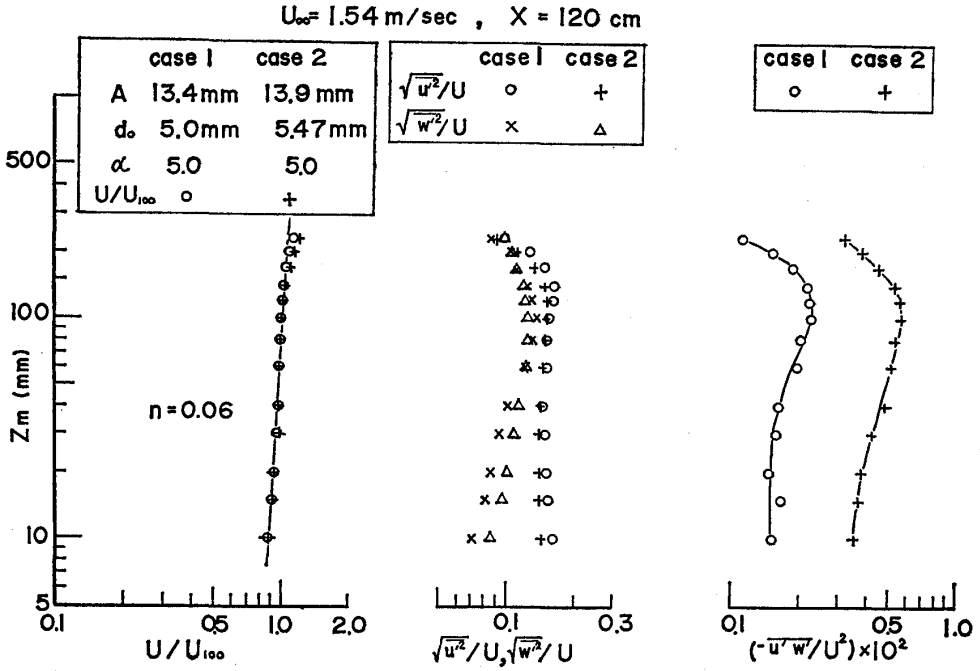

Fig. 8. Comparison of flow characteristics of two turbulent flows generated by two grids with different effective width of angle (The left side figure shows the vertical wind profiles, the middle one vertical distributions of turbulent intensities $\sqrt{\overline{u'^2}}/U$ and $\sqrt{\overline{w'^2}}/U$ and the right side one vertical distribution of vertical fluxes of momentum).

§ 7. Summary.

Determination of the empirical formula between the exponent n of the vertical wind profile expressed by the power law and the grid parameters A, d_0, α was made to find the practical method of constructing intentionally the grid to be desired under the conditions that n was independent of distance downwind from the grid (x) and tunnel velocity (U_∞) (it is confirmed experimentally). As the result the following equations were obtained for each case, that is,

(1) for the case of regular direction of angle

$$n=(0.055-0.0042\alpha)\left(\frac{d_0}{A}\right)^{-(0.11+0.103\alpha)}$$

$$\alpha<13,\quad 0.15\leqq\left(\frac{d_0}{A}\right)\leqq 0.45\quad\text{(limit of application)}$$

(2) for the case of reversed direction of angle

$$n=(0.034-0.0015\alpha)\left(\frac{d_0}{A}\right)^{-(0.65+0.098\alpha)}$$

$$\alpha<22,\quad 0.1\leqq\left(\frac{d_0}{A}\right)\leqq 0.5\quad\text{(limit of application)}$$

Hence, in the relationship as

$$\left(\frac{d_{m-1}}{d_0}\right)^{\alpha}(2A+d_0)=2\left(mA+\sum_{i=0}^{m-1}d_i\right)-d_{m-1}$$

which is derived from the exponential relation between spacing of angles and its height, when combination of A, d_0 and α which satisfies a value n to be desired is given and value of m are varied from 1 to $(m-1)$, each spacing d_{m-1} corresponding to each value of m can be successively obtained from the above equation and the grid to be desired may be constructed.

The model wind in the wind tunnel produced by this method was compared with the natural wind observed at Minnesota and it was found from this result that both mean wind profile and vertical distribution of turbulent intensity agreed well with each other respectively but the vertical distributions of vertical fluxes of momentum did not. However, it was found from the experimental result of two grids with the different effective width of angle that the agreement of vertical distributions of momentum fluxes could be expected by suitable combination of grid parameters.

Incidentally, a value of n produced by this method is at most about 0.11 at maximum in the case of regular direction of angle, on the contrary, considerably large value of n can be obtained by the use of equation (5) for the case of reversed direction of angle, however in this case turbulent intensity is relatively small as compared with the case of the use of equation (4). Hence if larger values of both n and turbulent intensity are required, other method must be considered.

This work was partially supported by the Grant-in-Aid for Special Project Research from the Ministry of Education, Science and Culture.

References

Adachi, T. and Kato, E., 1973: J. Japan Soc. Aero. Space Science, **21**, 573.

Armitt, J., 1966: The simulation of the atmospheric boundary layer in a wind tunnel. C.E.G.B., Lab. Note No. RD/L/N 83/66.

Bailey, A. and Vincent, N.D.G., 1943: Wind pressure on buildings, including effects of adjacent buildings. J. Instn. Civ. Engrs., **20**(8).

Baines, W.D. and Peterson, E.G., 1950: An investigation of flow through screens. Report of Iowa Institute of Hydraulics.

Baines, W.D., 1963: Effects of velocity distribution on wind loads and flow patterns on buildings. NPL International Conf. on Wind Effects on Buildings and Structures, London, England.

Cermak, J.E., 1958: Wind tunnel for the study of turbulence in the atmospheric surface layer. Dept. of Civil Engr., Colo. State Univ. Rpt. No. CER58JEC42, Ft. Collins, CO. 40p.

Counihan, J., 1969: An improved method of simulating an atmospheric boundary layer in a wind tunnel. Atmos. Envir., **3**, 197-214.

Davenport, A.G. and Isyumov, N., 1968: The application of the boundary layer wind tunnel to the prediction of wind loading. Proc. Int. Res. Sem. Wind Effects on Buildings and Structures, Ottawa, Can., vol. **1**, 201-230.

Hanafusa, T. and Fujitani, T., 1981: Characteristics of high wind (2). Preprint of the general meeting of Met. Soc. Japan, **39**, 84.

Izumi, Y. and Caughey, J.S., 1976: Minnesota 1973 Atmospheric Boundary Layer Experiment Data Report. AFCRL Environmental Research Papers, No. 547.

Jensen, M., 1958: The Model-Law for phenomena in natural wind. Ingenioren, International Edition 2.

Kato, M., 1982: An application of electrical filters to spectrum analysis. Pap. Met. Geophys., **33**(3), 137-147.

Lloyd, A., 1967: The generation of shear flow in a wind tunnel. Q.J. Roy. Met. Soc., **92**(395).

Nagib, H.M., Morkovin, M.V., Yung, J.T. and Tan-Atichat, J., 1974: On modeling of atmospheric surface layers by the counter-jet technique. AIAA Paper No. 74-638, AIAA 8th Aerodynamic Testing Conf., Bethesda, MD, Jul. 8-10, 9.

Nemoto, S., 1968: Similarity between natural local wind in the atmosphere and model wind in a wind tunnel. Pap. Met. Geophys., **19**(2), 131-230.

Ogawa, Y., 1976: A new wind tunnel for the simulation of atmospheric diffusion. Paper 76-17.07 pres. at 69th Ann. Mtg. of the APCA, June 27-July 1, Portland, OR.

Ogawa, Y., Diosey, P.G., Uehara, K. and Ueda, H., 1981: A wind tunnel for studying the effects of thermal stratification in the atmosphere. Atmos. Einvir., **15**(5), 807-821.

Owen, P.R. and Zienkiewicz, H.K., 1957: The production of uniform shear flow in wind tunnel. J. Fluid Mech., **2**, 521-531.

Plate, E.J. and Cermak, J.E., 1963: Micrometeorological wind tunnel facility-description and characteristics. Fluid Dynamics and Diffusion Lab. Rpt. CER63EJP-JEC9, Colo. State Univ., Ft. Collins, CO, 60p.

Sato, H., Onda, Y. and Saito, T., 1974: Laboratory simulation of atmospheric turbulence: Generation of arbitrary velocity distributions and model experiment on flow around Mt. Fuji. Adv. Geophys., vol. **18B**, 241-251.

Schon, J.P. and Mery, P., 1971: A preliminary study of the simulation of neutral atmospheric boundary layer using air injection in a wind tunnel. Atmos. Envir., **5**(5), 299-312.

Surry, D., 1967: Results of an experimental generation of large scale turbulence in a wind tunnel and its use in studying the turbulence effects on the aerodynamics of a rigid circular cylinder. NRC International Research Seminar: Wind Effects on Buildings and Structures, Ottawa.

Vickery, B. J., 1965: On the flow behind a coarse grid and its use as a model of atmospheric turbulence in studies related to wind loads on buildings. NPL Report 1143.

Yasueda, N., Tanaka, S. and Nemoto, S., 1980: The structure of turbulent flow over regularly arrayed rough surfaces (Wind Tunnel Experiment). Nat. Sci. Rep., Ochanomizu University, **31**(2), 81-91.